Protein J (2015) 34:220–235
DOI 10.1007/s10930-015-9616-z

Proteomic Analysis of Extracellular Vesicles Released by Adipocytes of Otsuka Long-Evans Tokushima Fatty (OLETF) Rats

Jeong-Eun Lee[1] · Pyong-Gon Moon[1] · In-Kyu Lee[2] · Moon-Chang Baek[1]

Published online: 22 May 2015

Abstract Extracellular vesicles (EVs) such as exosomes are secretory vesicles that act as autocrine, paracrine, or endocrine messengers; mediate intercellular cross-talk; and carry a cargo of various proteins. Because EVs can be transported to recipient cells via circulation, many researchers have been studying EVs from immune cells or cancer cells. Adipocytes are also considered endocrine cells and secrete adipokines such as adiponectin, regulating a variety of intracellular signaling pathways. Expansion of adipose tissue in obesity alters adipokine secretion, thereby increasing the risk of metabolic diseases. Characterization of adipocyte-derived exosomes is necessary to explain the communication between adipocytes and other cell types. In the present study, to identify proteins associated with adipocyte-derived exosomes, we isolated exosomes from adipose tissue of obese diabetic and obese nondiabetic rats. We identified proteins by analyzing exosomes from obese rats with type 2 diabetes and their matched control littermates using nano-liquid chromatography with tandem mass spectrometry coupled with label-free relative quantification. We identified 509 proteins from adipocytes including 81 known adipokines; ~78 % of all the identified proteins were categorized as exosome-associated proteins. Among the protein profiles, we uncovered 128 upregulated and 72 downregulated proteins, which are differentially expressed in OLETF adipocyte-derived exosomes. This study seems to demonstrate for the first time hundreds of proteins in exosomes released by adipocytes in obese rats and rats with type 2 diabetes. Thus, protein profiles of exosomes from adipocytes possibly indicate the transmission of signals as part of cell–cell communication and should further our understanding of obesity- and diabetes-related diseases.

Keywords Exosomes · Adipose · Adipokines · Obesity · Diabetes

Abbreviations

EVs	Extracellular vesicles
LETO	Long-Evans Tokushima Otsuka
OLETF	Otsuka Long-Evans Tokushima fatty
UPLC	Ultra-performance liquid chromatography
GPI	Glycophosphatidylinositol
TEM	Transmission electron microscope
NTA	Nanoparticle tracking analysis
TEABC	Triethylammonium bicarbonate
DDA	Data-dependent analysis

1 Introduction

Exosomes are released from various types of cells under both normal and pathological conditions and the size ranges from 50 to 150 nm. Exosomes are secreted by many types of cells including tumor cells [1], mast cells [2], and adipose cells [3]. Exosomes are now recognized as major

Electronic supplementary material The online version of this article (doi:10.1007/s10930-015-9616-z) contains supplementary material, which is available to authorized users.

✉ Moon-Chang Baek
mcbaek@knu.ac.kr

[1] Department Molecular Medicine, Cell and Matrix Research Institute, School of Medicine, Kyungpook National University, 101 Dongin-dong 2 Ga, Jung-Gu, Daegu 700-422, Republic of Korea

[2] Department Internal Medicine, Kyungpook National University, Daegu 700-422, Republic of Korea

mediators of intercellular communication, although they had previously been thought to be inert cell debris [4–6]. Because of these physiological characteristics, some researchers recently suggested that exosomes are promising disease biomarkers [7]. The mechanisms by which exosomes may mediate intercellular signaling involves the activation of receptors on the plasma membrane of the recipient cells or influx of exosomes into the recipient cells [4, 8]. Alternatively, exosomes may transmit signals to recipient cells by directly transferring bioactive molecules via vesicles. Furthermore, expanding efforts in the field of exosomes research may explain the interaction among endocrine organs. Moreover some authors have characterized exosomes from mouse adipose tissue [3], and 3T3-L1 adipocyte [9], and rat primary adipocytes secreting exosomes [10]. Exosome like vesicles that are released by adipocytes of *ob/ob* mice not only activate monocytes but also promote differentiation and proliferation of bone marrow-derived macrophages (BMDMs) [3]. In addition, lipid synthesis and storage in small adipocytes are stimulated by microvesicles from large adipocytes by transferring RNA and glycosylphophatidylinositol (GPI)-anchored proteins [11]. Recently, adiponectin, a well-known adipokine, was shown to be associated with exosomes in vivo [12] and was detected in the exosomes from murine adipocytes and adipose tissue using proteomic approach [3, 9]. Indeed, exosomes that are released from adipocytes may be present in the blood circulation [12]. Taken together, adipocytes-derived exosomes are involved in the development of metabolic diseases by mediating cell communications. Nonetheless, the function and characteristics of exosomes that are released from adipocytes during diabetes have yet to be elucidated.

Because obesity is frequently related with the development of metabolic diseases such as type 2 diabetes and vascular complications, it has become a global problem for health in the worldwide. Adipose tissue performs an endocrine function by producing signaling and mediator proteins known as adipokines, via which the adipose tissue communicates with other tissues and organs to maintain systemic homeostasis [13]. By secreting adipokines which mediate cell signaling, adipose tissue communicates with the liver, skeletal muscle, heart, brain, and vasculature [14, 15]. Recent data indicate that these adipokines constitute a complex interconnected network mediating the cross-talk among the above-mentioned tissues and organ. In obesity, expansion of adipose tissue has been implicated in inflammation of adipose tissue and in dysregulation of adipokine secretion. This chronic stage of inflammation indicates a crucial pathogenic connections between obesity and metabolic syndrome such as type 2 diabetes. Regional distribution of body fat also believed to be a major reliable risk factor of cardiovascular diseases [16]. In addition, biological role of adipose tissue is to produce physiologically active substances as well as to stores excess energy [17]. It is thought that visceral adipose tissue is involved in the pathogenesis of metabolic disorders and type 2 diabetes related complications [18]. Such signals converge on target tissues, for example, on the liver and affect glucose production or on beta cells of pancreas, thereby modulating insulin production. The genes that are up-regulated during adipocytic hypertrophy may participate in the development of obesity and its complications [19, 20]. Dysregulated production of adipokines contributes to the pathogenesis of obesity-associated metabolic syndrome. In order to identify proteins that are related to the progression of common diseases, various proteomic approaches have been used to characterize the secretome of rodent and human adipocytes and adipose tissues [21].

In this study, to identify adipocyte exosome-associated proteins, we used obese diabetic Otsuka Long-Evans Tokushima fatty (OLETF) rats and their counterparts, Long-Evans Tokushima Otsuka (LETO) rats as an experimental model [22, 23]. The OLETF rat represent a status of non-insulin dependent diabetes mellitus (NIDDM) by Kawano et al. [24]. Because OLETF rats show insulin resistance, obesity, hypertension, hyperinsulinemia, and hyperglycemia, they seem to be the most suitable animal for our study. The control strain LETO rats, which were derived from Long-Evans rats, are mostly healthy (never develop diabetes) but obese. We isolated adipose tissue from visceral fat and collected exosomes released by the adipocytes.

To identify the exosomal proteome in the adipocytes of obese rats and rats with type 2 diabetes, we used the nano-liquid chromatography with quantitative time-of-flight tandem mass spectrometry (nanoLC-Q-TOF–MS/MS) along with a label-free relative quantification method. We identified 509 proteins in adipocyte-derived exosomes, and some of the identified proteins were either known to be present in or were detected in mouse adipocytes. In addition, we compared protein expression between OLETF and LETO rats; we analyzed 128 upregulated and 72 down-regulated proteins, and changes in the expression of some of the differentially expressed proteins were confirmed by western blotting.

2 Materials and Methods

2.1 Animal Preparation

All experimental procedures were conducted in accordance with the Guidelines for Animal Experimentation of our institution. Four-week-old male OLETF and male LETO rats were obtained from Tokushima Research Institute of

Otsuka Pharmaceutical Co. (Tokushima) and maintained at an animal facility. The animals were fed standard chow until 32 weeks of age and kept at controlled temperature with a 12-h lighting cycle.

2.2 Isolation of Adipocytes and Primary Culture of Rat Adipocytes

Adipocytes were isolated by collagenase digestion from epididymal fat pads of male LETO ($n = 3$) and OLETF ($n = 3$) rats under sterile conditions according to procedures described previously [25]. The adipocytes were resuspended in 20 mL of adipocyte buffer (0.14 M NaCl, 4.7 mM KCl, 2.5 mM $CaCl_2$, 1.2 mM $MgSO_4$, 1.2 mM KH_2PO_4, 20 mM HEPES/KOH at pH 7.4) supplemented with 0.2 % (w/v) bovine serum albumin (BSA), 1 % antibiotic/antimycotic solution, and 1 mM sodium pyruvate, and incubated in a shaking water bath. Subsequently, the cells were washed by flotation with 50 mL of adipocyte buffer 3 times, then cells were resuspended in 10 mL of adipocyte buffer, and incubated. To minimize variation in the cell confluence and viability, the cells were subjected to washing step and flotation in same buffer. Adipocytes obtained from each rat (three rats per group) were cultured into individual dish.

2.3 Preparation of Adipocyte-Derived Exosomes

The cell culture medium was collected every 24 h for 3 days. The pooled conditioned medium (10 mL × 3 times = 30 mL) from each dish was subjected to serial centrifugations (Fig. 1): 300×*g* for 3 min, 1500×*g* for 15 min, and 3000×*g* for 15 min; after that, the medium was filtered through a membrane (0.2-μm pore) and centrifuged at 200,000×*g* for 1 h. For washing, we resuspended the pellet in PBS and then pelleted the EVs at 200,000×*g* for 1 h again. Exosomes were enriched in this pellet. The pellet was resuspended in PBS for further analysis. Total exosomal protein was quantified using the BCA protein assay (Thermo Fisher Scientific). Equal amount (1 μg) of exosomal proteins were used for each MS run, and equal amount (5 μg) of exosomal proteins were loaded on each lane of SDS-PAGE for western blot analysis (Fig. 1).

2.4 Electron Microscopy

The enriched exosomes were fixed in 4 % paraformaldehyde and deposited onto pure carbon-coated electron-microscope grids. The vesicle-coated grids were washed and incubated with 50 mM glycine in PBS. After staining with 3 % uranyl acetate, we dried the grids at room temperature and examined them at 6000× and 10,000× magnification under a transmission electron microscope (Hitachi H-7000).

2.5 Nanoparticle Tracking Analysis

Suspensions containing exosomes from the culture medium were analyzed using a Nano-Sight LM10 instrument (NanoSight). For the detection of particle size and concentration, a laser beam (wave length 405 nm) was passed through the dilute suspension of the EVs and the data were obtained in video recording. A video of 60-s duration was shot at the rate of 30 frames/s, and exosome movements were analyzed using the NTA software (version 2.2, NanoSight). NTA data acquisition settings were optimized at camera level 6–7, and detection threshold 5–6 for EV detection and kept constant during analysis of all samples, and acquired video was analyzed to obtain an estimate of the size distribution of isolated EVs.

2.6 Protein Digestion

The EV pellets from rat adipocytes were digested using the gel-assisted digestion method, as described previously [26, 27]. Briefly, the samples were mixed with acrylamide solution and solidified into gel, then cut into pieces, and washed with gel washing buffer (25 mM Triethylammonium bicarbonate (TEABC) in 50 % acetonitrile) 3 times, and dried. After drying, the proteins were treated with dithiothreitol (DTT) at 10 mM for reduction of disulfide bond, then treated with iodoacetamide (IAA) at 55 mM in the dark. The gel slices were washed and then dried. Trypsin (Promega) in TEABC was added (protein:trypsin 50:1) to gel and allowed to be soaked at 4 °C for 1 h, and then incubated at 37 °C overnight. The protein digestion was boosted by addition of enzyme again and followed by incubation for another 3 h. The peptides were extracted twice with buffer A (0.1 % formic acid/50 mM TEABC/50 % acetonitrile) and buffer B (0.1 % formic acid/50 mM TEABC) twice, in turn. These solutions were concentrated.

2.7 Mass Spectrometry

The digested samples were analyzed under optimized conditions as described previously [27]. Briefly, LC runs of the peptide mixtures of EV fractions were performed using a ultra-performance liquid chromatography (UPLC) (nanoAcquity system, Waters Corporation) equipped with a C18 trap column (5 μm, 20 mm × 180 μm) and a C18 analytical reversed-phase column (1.7 μm, 25 cm × 75 μm) (Waters Corporation). The separation of peptide samples were processed with a gradient 3–40 % of mobile phase B (0.1 % FA in acetonitrile) at 300 nL/min. The lock mass [Glu1-fibrinopeptide B solution was supplied through the

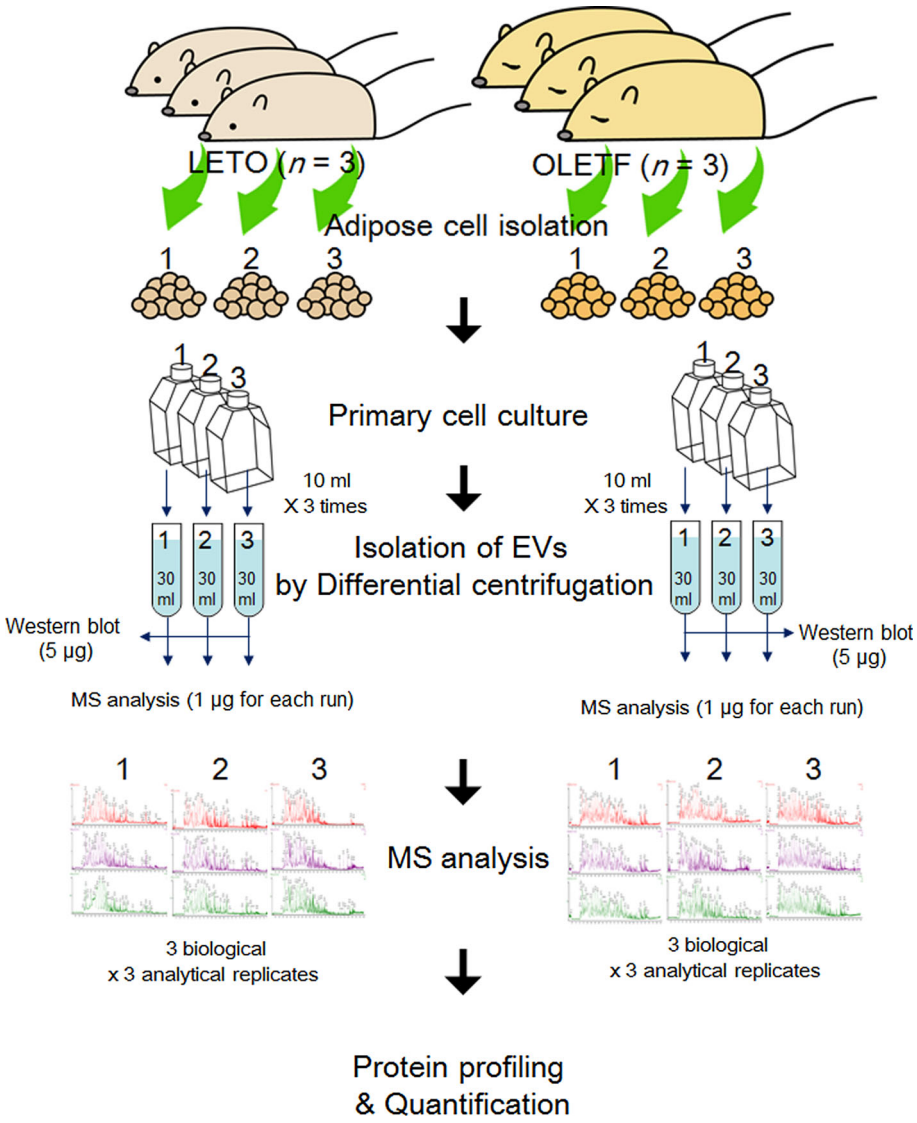

Fig. 1 A flow chart of the procedure Adipocytes were isolated from visceral adipose tissue of Long-Evans Tokushima Otsuka (LETO) rats ($n = 3$) and Otsuka Long-Evans Tokushima fatty (OLETF) rats ($n = 3$) and were cultured for 3 days. The culture medium was collected and centrifuged to enrich it in extracellular vesicles (EVs). The isolated EV fractions were analyzed using liquid chromatography with tandem mass spectrometry (LC-MS/MS). For protein profiling and protein quantification, the raw data files were processed in the MASCOT and IDEAL-Q software

reference spray of the NanoLockSpray source of the instrument and used for accurate mass detection. The peptide samples were analyzed using Q-TOF Premier mass spectrometer (Waters Corporation). The data acquisition was performed via data-dependent analysis (DDA) mode to automatically switch between the full MS scan (m/z 150–1600, 0.6 s) and the three MS/MS scans (m/z 100–1990, 0.2 s per scan) on the three most intense peaks.

2.8 Data Processing and Quantification

To create peak list file from MS raw data, MASCOT Distiller (Matrix Science; version 2.1) was used for DDA data. Subsequently, the data search of the MS/MS peak list files was performed in MASCOT (Matrix Science; version 2.2.1). MASCOT was set up to search against IPI_RAT_3.72 database, assuming trypsin as the digestion enzyme with 0.1 Da of parent ion tolerance and 0.05 Da of fragment ion mass tolerance. The modifications with carbamidomethylation of cysteine and oxidation of methionine as variable modification and the two missed cleavage of trypsin were allowed for analysis. Assignment of protein identification was determined when the protein identified using >2 peptides with >95 % probability or a single peptide with >99 % probability. During MASCOT analysis, each peak list data were performed and used for a search against a randomized decoy database which is automatically generated by MASCOT, that resulted in a <2 % false discovery rate according to decoy searches. For label-free quantification, the IDEAL-Q software (version 1.0.1.1) [28] was used. The raw data files from mass spectrometry were converted into files of mzXML using massWolf softwarer (Institute for Systems Biology). The search results were exported in the XML data format. In the data processing of IDEAL-Q, the identified proteins with

a score ≥34 were assigned for label-free quantification. To determine peptide abundance, the detected peptide peak cluster is processed by validation criteria (signal-to-noise, charge state, and isotopic distribution) as described previously [26, 28, 29]. If a peptide passes these validation, the peak cluster is used to construct peptide abundance. To quantify the relative peptide abundance, extracted ion chromatography (XIC) areas of an assigned peptide normalized by XIC area of internal standard were calculated. The relative protein ratio for each protein was resulted using average abundance among the corresponding peptides.

2.9 Western Blot

Protein extracts from EV fractions and cell were loaded to a polyacrylamide gel (8 %) and transferred to nitrocellulose membranes. Then the transferred membrane were incubated on a rotating shaker for 1 h in a blocking solution (5 % skim milk). After blocking, we incubated each blot overnight at 4 °C with a primary antibody. For validation of the differential expression of proteins, we used specific antibodies against CD63 (Abcam), caveolin (Abcam), lipoprotein lipase (Abcam), AQP7 (aquaporin 7; Abcam), AK2 (Santa Cruz Biotechnology), catalase (Abcam), and liver carboxylesterase (Abcam). Each blot was washed 3 times, followed by incubation with a secondary antibody (conjugated to horseradish peroxidase): a goat anti-mouse IgG antibody (Cell signaling) or a goat anti-rabbit IgG antibody (Santa Cruz Biotechnology). The blots were visualized with enhanced ECL detection reagents and ECL hyperfilm. For analysis of densitometry, the each blots was measured and normalized with CD63 for EV protein or GAPDH for cell lysates.

2.10 Statistical Analysis

The SPSS 17.0 software (IBM) was used for statistical analysis. The quantified ratios were calculated of 3 biological replicates per group and the p values were determined Student's t test between LETO and OLETF rats. For image analysis of western blot, Student's t test was used method if significance corresponded to $p < 0.05$ (mean ± SD, $n = 3$ to validate differences between LETO and OLETF rats).

3 Results

3.1 Isolation of Exosome from Cultured Adipocytes

To characterize proteins of adipocyte-derived EVs, we used the proteomic approach shown in the flow chart of Fig. 1. Two animal models of the disease: OLETF ($n = 3$) and matched control (LETO, $n = 3$) rats served as a source of adipose cells in this study. The isolated adipocytes from single rat were cultured into one dish, and the culture medium of each dish was pooled every 24 h during 3 days to isolate the adipocyte-derived exosomes. The EV fractions were prepared by modified differential ultracentrifugation method from previously described method [30]; to further confirm the presence of exosomes after the centrifugation, we immunoblotted each fraction (obtained using the differential centrifugation method shown in Fig. 2a, top) for CD63, an exosome marker protein [31]. The immunoblot results showed that the exosomes were enriched in the pellet after centrifugation at 200,000×g. To evaluate the size of the isolated EVs, we measured the vesicle size using NanoSight. The isolated adipocyte-derived EVs had a known exosome size that ranged between 50 and 150 nm (Fig. 2b). The isolated vesicles were then analyzed by transmission electron microscopy (Fig. 2c); the images showed that our exosome preparations contained vesicles that were surrounded by a lipid bilayer and had a diameter of ~100 nm. Taken together, our results indicated that the majority of the EV fractions prepared by differential ultracentrifugation were enriched in exosomes.

3.2 Protein Profiling of Adipocyte Exosomes

Each EV fraction from adipose cells of LETO rats ($n = 3$) and OLETF rats ($n = 3$) was used for the proteomic analysis. Lysed samples from each group were used for gel-assisted digestion and were assessed by LC–MS/MS analysis in triplicate. 276, 257, and 252 proteins from LETO group, and 279, 280, and 312 proteins from OLETF group were identified ($p < 0.05$, protein score ≥34, false discovery rate <1 %). To identify whole of EV proteins from adipocyte, we combined all of data from MS runs (3 biological × 3 analytical replicates of each group = 18 runs in Fig. 1 and Supplementary Table 1), resulting in the identification of 509 non-redundant proteins. Protein profiles were compared to the entries in the ExoCarta database; we found that approximately 78 % of the identified proteins were listed in the database (Fig. 3a). Using the DAVID gene ontology-based functional annotation analysis, the identified proteins were categorized by their subcellular location (Fig. 3b). According to the classification by subcellular locations, plasma membrane and extracellular-space proteins constituted a half of the exosomal content. In addition, the protein identification revealed 44 % of cytosolic proteins and 5 % of nuclear proteins. Seven functional clusters were built by the DAVID annotation tool from our 509 identified proteins: the first cluster corresponded to developmental processes, the second to localization, the third to establishment of localization, the fourth to organization of cellular components, the fifth to metabolic processes, the sixth to biogenesis of cellular

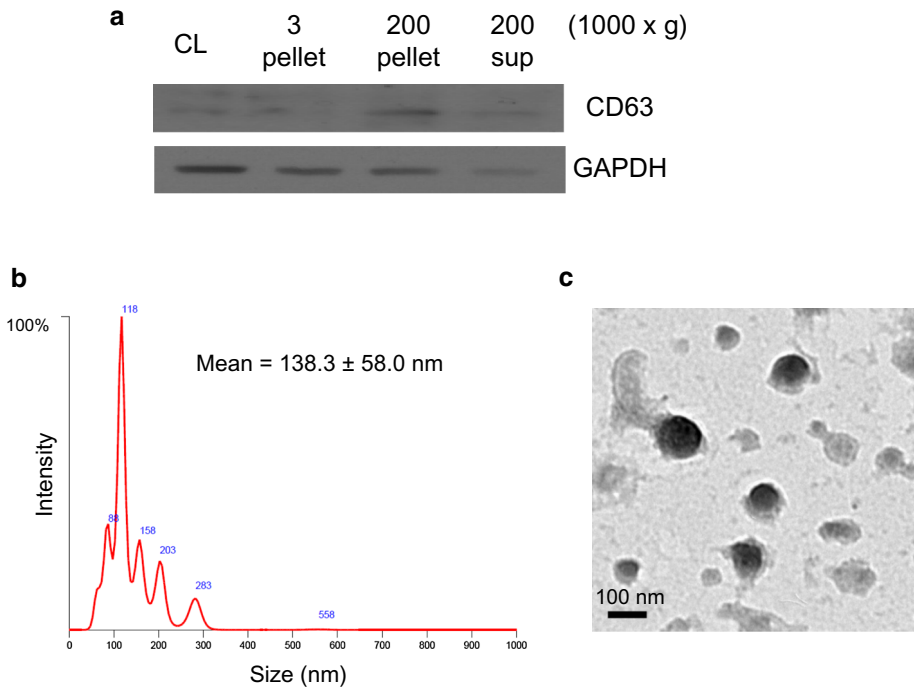

Fig. 2 Characterization of the isolated extracellular vesicles (EVs). **a** The pellets after centrifugation at 3000×*g* and 200,000×*g* and the supernatant after centrifugation at 200,000×*g* (the differential centrifugation method) as well as cell lysates (CL) were separated in an 8 % polyacrylamide gel and transferred onto a membrane. The transferred blots were immunoblotted with an anti-CD63 or anti-GAPDH antibody. **b** The distribution of vesicle sizes in the 200,000×*g* pellet was measured using NanoSight NTA software. **c** Representative images of transmission electron microscopy of EVs from adipocytes of Otsuka Long-Evans Tokushima fatty (OLETF) rats. The *scale bar* is 100 nm

components, and seventh cluster corresponded to cellular processes (Fig. 3c). The molecular functions of the identified proteins indicated that the exosomes contained diverse types of proteins such as transporters, antioxidants, electron carriers, enzymes, and structural molecules (Fig. 3d). We also compared our results to another study where the authors analyzed human-adipocytic-secretory-adipokine profiles using LC–MS/MS [21]. Eighty-one proteins, including adiponectin, fatty acid synthase, and catalase among the identified exosome-associated proteins were identified as adipokines in that profiling study [21] (Supplementary Table 2). Additionally, several adipose-tissue-specific proteins were successfully identified here in the EV fraction: carboxylesterase 3, caveolin 1, fatty acid-binding protein 4 (FABP4), and lipase (hormone-sensitive). FABP4, an adipokine which plays a crucial role in the pathogenesis of chronic metabolic diseases, was identified in the secretome of 3T3-L1 adipocytes in our previous study [32]; a recent study showed that this protein is secreted from adipocytes through secretory vesicles [33].

3.3 Quantification of Identified Proteins

For quantification of disease-related proteins from the exosomes, the 509 identified proteins were quantified using the IDEAL-Q software (version 1.0.6.2) for label-free relative quantification as we have described previously [26]. To analyze the differentially expressed adipocytic-exosome-associated proteins, we quantified 3 replicates per group in IDEAL-Q. The cutoff levels that we determined for the differentially expressed proteins were filtered if the p value <0.05 and to 2 coefficients of variation (CV) of the relative protein ratio. In this experiment, 2 CV equaled 24.8 %, resulting a 1.2-fold change. According to these criteria, 165 proteins were expressed significantly differentially between OLETF and LETO rats. The resulting upregulated (128 entries) and downregulated proteins (72 entries) in the exosomes are listed in Table 1.

3.4 Validation of Quantified Proteins Between LETO and OLETF

To characterize exosomal proteins from adipocytes of LETO and OLETF rats, we used western blotting to confirm the relative amounts of differentially expressed proteins of interest in exosomes and cultured-adipose-tissue lysates. Depending on the available commercial antibodies, and according to bioinformatic tools such as Gene Ontology Biological Process and Molecular Function annotation and some literature, we selected 6 proteins for further validation considering their involvement in obesity, type 2 diabetes, or lipid metabolism. These were (1) caveolin 1, which plays a role in vesicular transport and cholesterol homeostasis; (2) lipoprotein lipase, which participates in the metabolism and transport of lipids; (3) aquaporin 7 (AQP7), which modulates glycerol permeability of adipocytes by controlling triglyceride accumulation and fat-cell size; (4) adenylate kinase 2 (AK2), which may perform an important function in energy

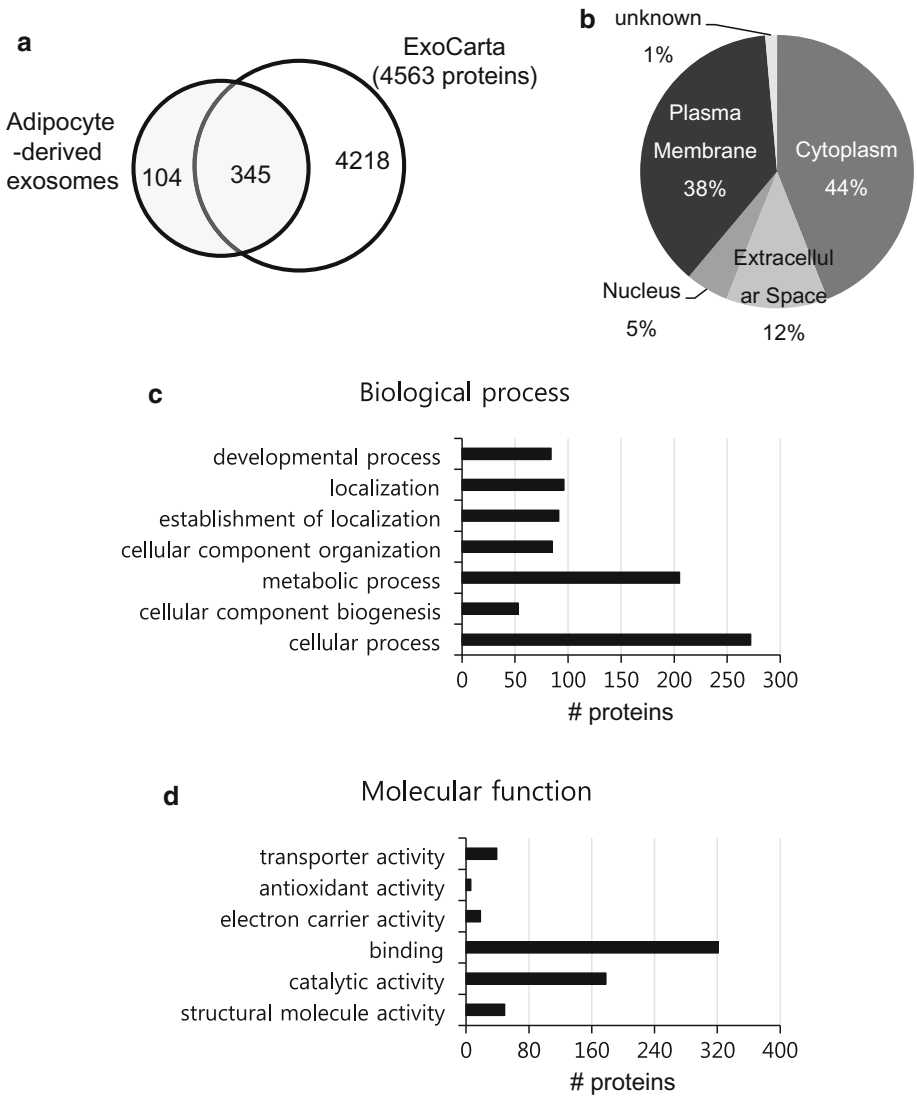

Fig. 3 Characterization and classification of the identified proteomic profiles of adipocyte-derived exosomes.
a Comparison of the identified proteins with entries in the ExoCarta database. Using gene ontology analysis (DAVID; web-based bioinformatic analysis tool), we calculated the percentage of proteins or the number of proteins, by
b subcellular location,
c molecular function, or
d biological process

homeostasis in mature adipocytes; (5) catalase, which is an antioxidant enzyme; and (6) liver carboxylesterase, which controls cellular cholesterol esterification levels and detoxification. In the western blot analysis shown in Fig. 4, protein expression levels of caveolin 1, lipoprotein lipase, and aquaporin 7 were significantly higher in exosomes and cells of OLETF rats than in those of LETO rats. In contrast, AK2, catalase, and liver carboxylesterase were expressed more weakly in OLETF rats than in LETO rats. The upregulation or downregulation of proteins were confirmed to be similar between the exosomal fraction and the tissue lysate, even though the protein fold change in the densitometric analysis showed slight differences between the exosomes and the lysate of the tissue of origin. In addition, our western blot analysis showed similarity of protein expression changes between the exosomal fraction and the tissue lysate according to protein quantification analyses in IDEAL-Q; this result suggested that the findings of our nanoLC–MS/MS analysis provided reliable disease-related proteomic profiling.

4 Discussion

The importance of exosome secretion and the release of proteins from the cell has now been established in many cell types and under various physiological conditions, for example, during bone growth, platelet activation, immune responses, and especially in the tumor microenvironment. It is likely that the released exosomes carry a variety of cell-derived information and perform active functions. Adipose tissue produces various biologically active molecules collectively known as adipokines, e.g., adiponectin and FABP4 (adipocyte lipid-binding protein) [21]. Because adipose tissue may be involved in endocrine disorders, especially diabetes (which presents with aberrations in

Table 1 Statistically significant proteins that were found to be expressed differentially between adipocytic exosomes of Otsuka Long-Evans Tokushima fatty (OLETF) rats and Long-Evans Tokushima Otsuka (LETO) rats

AccNo	Protein description	OLETF/ LETO ratio	Quantification *p* value
IPI00231694	Xdh Xanthine dehydrogenase/oxidase	0.35	5.70E−07
IPI00202370	Maoa Amine oxidase [flavin-containing] A	0.46	6.58E−05
IPI00196661	Ywhaq 14-3-3 protein theta	0.50	1.01E−02
IPI00207355	Hspa2 Heat shock-related 70 kDa protein 2	0.52	8.96E−04
IPI00204774	**Cesl Liver carboxylesterase B-1**	**0.53**	**1.19E−09**
IPI00231742	**Cat Catalase**	**0.57**	**3.29E−05**
IPI00209082	Actn1 Alpha-actinin-1	0.57	1.32E−04
IPI00764167	Myh11 similar to Myosin-11 (Myosin heavy chain, smooth muscle isoform) (SMMHC) isoform 3	0.58	4.33E−04
IPI00209115	Slc25a3 Solute carrier family 25 (Mitochondrial carrier)	0.60	6.02E−03
IPI00851130	Gda Guanine deaminase	0.60	4.86E−05
IPI00454475	Krt77 Keratin, type II cytoskeletal 1b	0.61	6.82E−03
IPI00363849	Lamc1 laminin, gamma 1	0.62	4.87E−03
IPI00371853	Col6a1 similar to Collagen alpha-1(VI) chain precursor	0.62	1.41E−02
IPI00212868	Lamb2 Laminin subunit beta-2	0.64	6.38E−03
IPI00215564	Rab7a Ras-related protein Rab-7a	0.64	3.46E−04
IPI00200013	Prkaca Isoform 1 of cAMP-dependent protein kinase catalytic subunit alpha	0.65	5.79E−03
IPI00187747	Rap1a Ras-related protein Rap-1A	1.50	9.46E−03
IPI00211225	Acadl Long-chain specific acyl-CoA dehydrogenase, mitochondrial	1.50	5.24E−03
IPI00515821	Aoc3 Membrane primary amine oxidase	1.50	3.75E−02
IPI00324741	Pdia3 Protein disulfide-isomerase A3	1.51	1.89E−02
IPI00231674	Arf3 ADP-ribosylation factor 3	1.53	1.32E−02
IPI00204703	Serpinh1 Serpin H1	1.53	3.55E−03
IPI00396910	Atp5a1 ATP synthase subunit alpha, mitochondrial	1.53	1.69E−02
IPI00211756	Phb Prohibitin	1.56	3.93E−02
IPI00464670	Capg Macrophage-capping protein	1.57	2.89E−02
IPI00393867	Myo1c Myosin-Ic	1.62	2.35E−03
IPI00363708	RGD1564709 ATP-binding cassette, sub-family G (WHITE), member 3 family member	1.63	3.32E−02
IPI00475639	Tubb2a Tubulin beta-2A chain	1.63	5.61E−02
IPI00189690	Rab8b Ras-related protein Rab-8B	1.63	2.77E−03
IPI00388015	Coro1c coronin, actin binding protein 1C	1.66	2.84E−03
IPI00365985	Tra1 Isoform 1 of Endoplasmin	1.66	8.87E−03
IPI00231197	Cd36 Platelet glycoprotein 4	1.67	1.30E−02
IPI00211968	Map3k12 Mitogen-activated protein kinase kinase kinase 12	1.68	3.81E−02
IPI00365286	Vcl Vinculin	1.70	2.85E−02
IPI00199636	Canx Calnexin	1.70	3.01E−03
IPI00551812	Atp5b ATP synthase subunit beta, mitochondrial	1.70	1.03E−02
IPI00206948	Retsat All-trans-retinol 13,14-reductase	1.71	1.87E−03
IPI00763910	LOC684747 similar to 60 kDa heat shock protein, mitochondrial precursor	1.72	5.02E−02
IPI00766788	Oxct1 Succinyl-CoA:3-ketoacid-coenzyme A transferase 1, mitochondrial	1.72	4.40E−02
IPI00209480	Pccb Propionyl-CoA carboxylase beta chain, mitochondrial	1.73	2.86E−02
IPI00339167	Tuba1b Tubulin alpha-1B chain	1.73	4.82E−02
IPI00360340	Ehd1 EH domain-containing protein 1	1.73	2.01E−03
IPI00366293	Tst Thiosulfate sulfurtransferase	1.74	7.25E−04
IPI00870881	Ilvbl ilvB (bacterial acetolactate synthase)-like	1.74	4.40E−05
IPI00197344	Mgll Monoglyceride lipase	1.74	1.20E−04

Table 1 continued

AccNo	Protein description	OLETF/ LETO ratio	Quantification *p* value
IPI00212622	Hadha Trifunctional enzyme subunit alpha, mitochondrial	1.75	3.84E−02
IPI00206624	Hspa5 78 kDa glucose-regulated protein	1.77	2.17E−03
IPI00211448	Ehd2 EH domain-containing protein 2	1.78	2.98E−03
IPI00230986	Rtn4 Isoform 2 of Reticulon-4	1.78	1.56E−06
IPI00190943	Gfap Isoform 1 of Glial fibrillary acidic protein	1.78	1.48E−02
IPI00557688	−28 kDa protein	1.79	8.65E−04
IPI00189471	**Lpl Lipoprotein lipase**	**1.81**	**2.02E−02**
IPI00364311	Gpi Glucose-6-phosphate isomerase	1.82	1.49E−02
IPI00200466	Slc25a5 ADP/ATP translocase 2	1.84	1.36E−03
IPI00198887	P4hb Protein disulfide-isomerase	1.88	2.13E−02
IPI00831745	Anxa6 annexin A6	1.90	1.50E−03
IPI00365600	Prkar2b cAMP-dependent protein kinase type II-beta regulatory subunit	1.94	2.07E−02
IPI00201333	Ganab 107 kDa protein	1.94	3.89E−04
IPI00213644	Ppib Peptidyl-prolyl cis–trans isomerase B	2.00	2.45E−02
IPI00193983	Cltc Clathrin heavy chain 1	2.05	2.95E−02
IPI00190020	Atp2a2 Isoform SERCA2B of Sarcoplasmic/endoplasmic reticulum calcium ATPase 2	2.10	1.23E−02
IPI00197994	Agpat2 1-acylglycerol-3-phosphate O-acyltransferase 2	2.11	1.20E−03
IPI00205978	−100 kDa protein	2.13	9.08E−03
IPI00364948	Aldh3a2 Fatty aldehyde dehydrogenase	2.15	4.13E−03
IPI00339148	Hspd1 60 kDa heat shock protein, mitochondrial	2.15	5.34E−02
IPI00339197	Pkm2 Isoform M2 of Pyruvate kinase isozymes M1/M2	2.24	1.45E−02
IPI00231475	H3f3b Histone H3.3	2.26	1.24E−02
IPI00365929	Pdia6 protein disulfide-isomerase A6	2.28	6.07E−03
IPI00364884	Ssr1 Translocon-associated protein subunit alpha	2.29	2.56E−03
IPI00886474	Rps5 Rps5 protein	2.34	3.96E−05
IPI00231139	Tkt transketolase	2.43	2.95E−02
IPI00206434	Lnpep Leucyl-cystinyl aminopeptidase	2.44	3.98E−04
IPI00201494	Erlin2 Erlin-2	2.52	4.72E−02
IPI00230956	Slc1a3 Isoform GLAST-1A of Excitatory amino acid transporter 1	2.58	2.49E−03
IPI00208495	−33 kDa protein	2.65	2.27E−03
IPI00192313	**Cav1 Isoform Alpha of Caveolin-1**	**2.65**	**7.29E−06**
IPI00213458	Surf4 surfeit 4	2.68	9.54E−04
IPI00325189	Nme2 Nucleoside diphosphate kinase B	2.82	1.08E−02
IPI00382191	Pgd 6-phosphogluconate dehydrogenase, decarboxylating	2.86	7.50E−03
IPI00365423	Ppp2r1a Protein phosphatase 2 (Formerly 2A), regulatory subunit A (PR 65), alpha isoform, isoform CRA_a	2.95	7.64E−05
IPI00886470	Hsd17b10 3-hydroxyacyl-CoA dehydrogenase type-2	3.01	4.96E−02
IPI00189217	−38 kDa protein	3.31	1.54E−03
IPI00393561	Slc1a5 Solute carrier family 1 (Neutral amino acid transporter), member 5, isoform CRA_b	3.39	8.68E−03
IPI00188059	Rpn2 Dolichyl-diphosphooligosaccharide–protein glycosyltransferase subunit 2	3.50	3.61E−03
IPI00360363	Atl3 Isoform 1 of Atlastin-3	3.91	3.43E−03
IPI00421508	Cav2 Caveolin-2	3.93	1.21E−03
IPI00947772	Aldh3a2 48 kDa protein	4.15	2.93E−03
IPI00191170	Dgat1 Diacylglycerol acyltransferase	4.28	2.86E−03
IPI00362182	Lipe Isoform 1 of Hormone-sensitive lipase	5.96	2.28E−02
IPI00914294	Anxa13 annexin A13	6.53	2.45E−04

Table 1 continued

AccNo	Protein description	OLETF/ LETO ratio	Quantification *p* value
IPI00364431	Sucla2 succinate-Coenzyme A ligase, ADP-forming, beta subunit	8.80	1.27E−15
IPI00764690	Mtch2 mitochondrial carrier homolog 2	12.28	8.86E−02
IPI00231136	Nid1 similar to Nidogen-1 precursor	LETO	1.25E−03
IPI00200271	Ehd4 Pincher	LETO	1.25E−03
IPI00869578	Loxl4 lysyl oxidase-like 4	LETO	1.25E−03
IPI00948445	Lama4 laminin, alpha 4	LETO	5.06E−03
IPI00198717	Mdh1 Malate dehydrogenase, cytoplasmic	LETO	5.07E−03
IPI00948172	Sncg 13 kDa protein	LETO	5.07E−03
IPI00421332	LOC306079 LRRGT00066	LETO	7.17E−03
IPI00208215	Prdx3 Thioredoxin-dependent peroxide reductase, mitochondrial	LETO	7.17E−03
IPI00464827	G6pc3 Glucose-6-phosphatase 3	LETO	1.66E−02
IPI00324633	Glud1 Glutamate dehydrogenase 1, mitochondrial	LETO	2.02E−02
IPI00203214	Eef2 Elongation factor 2	LETO	2.02E−02
IPI00212776	Rps3 40S ribosomal protein S3	LETO	2.02E−02
IPI00361301	Lama2 similar to Laminin alpha-2 chain precursor	LETO	2.62E−02
IPI00230857	**Ak2 Isoform 1 of Adenylate kinase 2, mitochondrial**	**LETO**	**2.62E−02**
IPI00205166	Itga6 similar to integrin alpha 6 isoform 2	LETO	2.62E−02
IPI00191142	Rps10 40S ribosomal protein S10	LETO	2.62E−02
IPI00205745	Prdx5 Isoform Mitochondrial of Peroxiredoxin-5, mitochondrial	LETO	2.62E−02
IPI00782681	−121 kDa protein	LETO	2.62E−02
IPI00200257	Cdh13 T-cadherin	LETO	2.62E−02
IPI00231202	Rps8 40S ribosomal protein S8	LETO	2.62E−02
IPI00197077	Ppp2r2d Serine/threonine-protein phosphatase 2A 55 kDa regulatory subunit B delta isoform	LETO	2.62E−02
IPI00373752	Flnb 278 kDa protein	LETO	2.62E−02
IPI00557975	Acad11 Acyl-CoA dehydrogenase family member 11	LETO	2.77E−02
IPI00471762	Sypl1 Synaptophysin-like protein, isoform CRA_a	LETO	2.77E−02
IPI00189773	Acadsb Short/branched chain specific acyl-CoA dehydrogenase, mitochondrial	LETO	3.84E−02
IPI00208205	Hspa8 Heat shock cognate 71 kDa protein	LETO	3.84E−02
IPI00195173	Cd59 CD59 glycoprotein	LETO	5.66E−02
IPI00231767	Tpi1 Triosephosphate isomerase	LETO	5.66E−02
IPI00560492	Prkacb 46 kDa protein	LETO	N/A
IPI00765963	RGD1307220 similar to alpha 3 type VI collagen isoform 1 precursor	LETO	N/A
IPI00211128	Tspo Translocator protein	LETO	N/A
IPI00362106	Fermt2 RCG61183, isoform CRA_b	LETO	N/A
IPI00370711	Epx eosinophil peroxidase	LETO	N/A
IPI00551702	Dlst Dihydrolipoyllysine-residue succinyltransferase component of 2-oxoglutarate dehydrogenase complex, mitochondrial	LETO	N/A
IPI00190088	Postn 90 kDa protein	LETO	N/A
IPI00187731	Tpm2 Isoform 2 of Tropomyosin beta chain	LETO	N/A
IPI00197568	Gdi2 Rab GDP dissociation inhibitor beta	LETO	N/A
IPI00203481	LOC687680;LOC691716 similar to ribosomal protein S15a	LETO	N/A
IPI00421451	Rps16 similar to 40S ribosomal protein S16	LETO	N/A
IPI00202512	Rpl4 60S ribosomal protein L4	LETO	N/A
IPI00566489	RGD1309707 hypothetical protein LOC690516	LETO	N/A
IPI00202543	Hk1 Hexokinase-1	LETO	N/A
IPI00214561	Lims1 46 kDa protein	LETO	N/A
IPI00780672	Kb23 Type II keratin Kb23	LETO	N/A

Table 1 continued

AccNo	Protein description	OLETF/ LETO ratio	Quantification *p* value
IPI00421797	Krt35 Type I hair keratin KA30	LETO	N/A
IPI00212499	Iyd Iodotyrosine dehalogenase 1	LETO	N/A
IPI00211593	Sod2 Superoxide dismutase [Mn], mitochondrial	LETO	N/A
IPI00230838	Atp5h ATP synthase subunit d, mitochondrial	LETO	N/A
IPI00778460	Lama2 141 kDa protein	LETO	N/A
IPI00209045	Acox3 76 kDa protein	LETO	N/A
IPI00366218	Cct2 T-complex protein 1 subunit beta	LETO	N/A
IPI00949810	Myo1c 122 kDa protein	LETO	N/A
IPI00359223	Kif13a 190 kDa protein	LETO	N/A
IPI00188666	Krt27 Keratin, type I cytoskeletal 27	LETO	N/A
IPI00231445	Rpl15 60S ribosomal protein L15	LETO	N/A
IPI00370813	Morc4 similar to MORC family CW-type zinc finger 4	LETO	N/A
IPI00195123	Atp5o ATP synthase subunit O, mitochondrial	OLETF	3.11E−05
IPI00210494	Sts Steryl-sulfatase	OLETF	1.01E−04
IPI00326305	Atp1a1 Sodium/potassium-transporting ATPase subunit alpha-1	OLETF	1.02E−04
IPI00231966	Arf4 ADP-ribosylation factor 4	OLETF	1.11E−03
IPI00194688	Tmem120a Transmembrane protein 120A	OLETF	2.75E−03
IPI00196994	Arhgdia Rho GDP-dissociation inhibitor 1	OLETF	2.75E−03
IPI00213436	Ndufa4 RCG28086, isoform CRA_a	OLETF	5.07E−03
IPI00206010	Rras Harvey rat sarcoma virus oncogene, subgroup R	OLETF	5.07E−03
IPI00231359	Acads Acetyl-Coenzyme A dehydrogenase, short chain, isoform CRA_a	OLETF	5.07E−03
IPI00215190	Fkbp9 Peptidyl-prolyl cis–trans isomerase FKBP9	OLETF	5.07E−03
IPI00422076	Thbs1 Thrombospondin 1	OLETF	5.07E−03
IPI00851119	Ptprk Receptor-like protein tyrosine phosphatase kappa	OLETF	7.61E−03
IPI00207038	Kb15 Type II keratin Kb15	OLETF	2.02E−02
IPI00764098	Ccdc109a coiled-coil domain containing 109A	OLETF	2.61E−02
IPI00372458	Copa Copa protein	OLETF	2.62E−02
IPI00199641	Gcs1 Mannosyl-oligosaccharide glucosidase	OLETF	2.62E−02
IPI00364046	Tuba1c Tubulin alpha-1C chain	OLETF	5.66E−02
IPI00230868	Gnaq Guanine nucleotide-binding protein G(q) subunit alpha	OLETF	6.64E−02
IPI00191397	Nedd4 l similar to E3 ubiquitin-protein ligase NEDD4-like protein	OLETF	6.64E−02
IPI00364616	RGD1309676 Uncharacterized protein C10orf58 homolog	OLETF	7.36E−02
IPI00421718	Rpl22 60S ribosomal protein L22	OLETF	N/A
IPI00212220	Pdia4 Protein disulfide-isomerase A4	OLETF	N/A
IPI00188330	Ndufs8 Ndufs8 protein	OLETF	N/A
IPI00421780	Krt73 Keratin, type II cytoskeletal 73	OLETF	N/A
IPI00421506	Rtn3 Rtn3 protein	OLETF	N/A
IPI00196965	Abhd12 Monoacylglycerol lipase ABHD12	OLETF	N/A
IPI00373433	Cenpe similar to centromere protein E	OLETF	N/A
IPI00409539	Flna 281 kDa protein	OLETF	N/A
IPI00371339	Ano10 similar to CG15270-PA, isoform A	OLETF	N/A
IPI00210062	Sncg Gamma-synuclein	OLETF	N/A
IPI00566938	RGD1565804 similar to alpha 3 type VI collagen isoform 1 precursor	OLETF	N/A
IPI00365784	Aspn Asporin	OLETF	N/A
IPI00230987	Rtn4 Isoform 3 of Reticulon-4	OLETF	N/A
IPI00201500	Rps14 40S ribosomal protein S14	OLETF	N/A
IPI00421812	Krt76 Type II keratin Kb9	OLETF	N/A

Table 1 continued

AccNo	Protein description	OLETF/ LETO ratio	Quantification *p* value
IPI00914772	Adck5 aarF domain containing kinase 5	OLETF	N/A
IPI00205519	Ugcgl1 UDP-glucose:glycoprotein glucosyltransferase 1	OLETF	N/A
IPI00202616	Ndufs3 NADH dehydrogenase (ubiquinone) Fe-S protein 3	OLETF	N/A
IPI00285606	Cdc42 Isoform 1 of Cell division control protein 42 homolog	OLETF	N/A
IPI00200070	Nucb2 Nucleobindin-2	OLETF	N/A
IPI00382320	RGD1311563 RGD1311563 protein	OLETF	N/A
IPI00421762	C1rl Complement C1r subcomponent-like protein	OLETF	N/A
IPI00213597	Ucn Urocortin	OLETF	N/A
IPI00192503	**Aqp7 Aquaporin-7**	**OLETF**	N/A
IPI00210116	Lman1 Protein ERGIC-53	OLETF	N/A
IPI00212731	Ctsd Cathepsin D	OLETF	N/A
IPI00365542	Lamb1 Protein	OLETF	N/A
IPI00324020	Glul Glutamine synthetase	OLETF	N/A
IPI00422037	C4-2 complement component 4, gene 2	OLETF	N/A
IPI00358313	Plp2 Proteolipid protein 2	OLETF	N/A
IPI00192912	Rcn1 reticulocalbin 1, EF-hand calcium binding domain	OLETF	N/A
IPI00337168	Cct4 T-complex protein 1 subunit delta	OLETF	N/A

The *p* values were determined using Student's *t* test, and the ratios were calculated using the ion chromatography (XIC) area of 3 replicates per group in the IDELA-Q software. The 6 proteins that were selected for validation are shown in boldface

N/A, Non-available, indicates unique proteins detected in that group not in another group

many organs), one possible cause of endocrine disorders may involve secreted microvesicles including exosomes derived from a primary disease organ. It has been demonstrated that the para-/endocrine regulation of adipocyte-derived extracellular vesicles, including exosomes and microvesicles that contain active mRNAs and proteins, entails a transfer of these vesicles to other cells and stimulation of intracellular communication during such processes as macrophage activation [3], angiogenesis [34], and lipid synthesis [9, 35].). Moreover, recent studies showed that in human hepatocarcinoma HepG2 cells, dysfunction of the TGF-β signaling pathway can be induced by exosomes from obesity-related adipocytes but not by exosomes from lean-tissue adipocytes [36]. Those authors hypothesized that the hepatocyte dysfunction can be induced by exosomes from visceral adipose tissue of obese patients; this was a novel paradigm for obesity-related liver diseases. By analyzing protein profiles of exosomes derived from adipocytes in present study, we confirmed the results of other studies that tested the possibility that adipocyte-derived exosomes participate in communication with other cell types.

One of the main aims of our study was to identify the proteome of extracellular vesicles from adipocytes of LETO and OLETF rats because this information may help to determine disease-related functions of exosomes in this animal model of diabetes. To date, proteomic analyses involving diabetic OLETF rats have been focused on the tissue proteome or oxidative stress-related protein modifications such as carbonylation, in comparison with LETO rats [37, 38]. Various studies involving 2-dimensional PAGE with LC–MS/MS as a targeted proteomic approach were designed to identify high-molecular-mass proteins with modifications in various tissues [38, 39]. As a result, several meaningful carbonyl proteins were identified, which show differential expression in comparison with LETO rats. On the other hand, we identified a great variety of proteins using our nanoLC–MS/MS coupled with relative quantitative proteomics. For the first time, proteomic analysis of adipocyte-derived exosomes was performed in both a diabetes animal model (OLETF rats) and controls (LETO rats) using LC–MS/MS. A total of 81 proteins, including adiponectin from adipocyte-derived exosomes, were identified previously by means of high-throughput proteomic analysis of adipokines from human primary adipocytes [21]. In fact, some in vivo studies have shown that there is an association of adiponectin to blood-circulating exosomes in genetically obese mice (*ob/ob*) and the corresponding lean mice (wild-type) [12]. Those researchers found that adiponectin concentrations in the circulating exosomes between the lean mice and obese mice shows no differences. In contrast, the ratio of adiponectin concentration to protein amount in the exosome is significantly lower in *ob/ob* mice than in wild-type mice [12]. Similarly, in the present study, there is no significant difference between LETO and OLETF rats in adiponectin

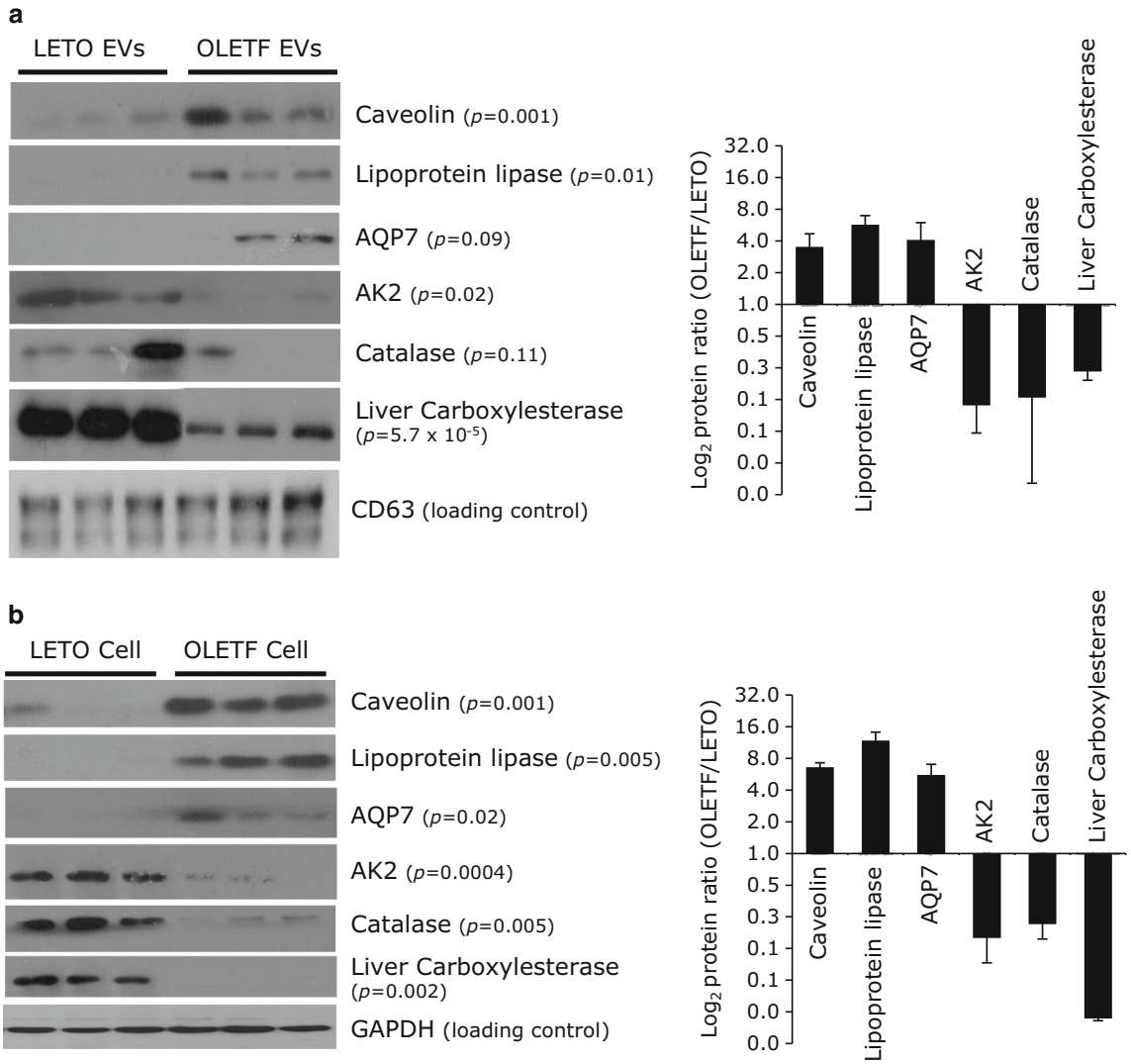

Fig. 4 Validation of the proteins that were expressed differentially between Otsuka Long-Evans Tokushima fatty (OLETF) rats and Long-Evans Tokushima Otsuka (LETO) rats. The expression levels of some upregulated or downregulated proteins were confirmed in the fraction of adipocyte-derived extracellular vesicles (EVs) (**a**) and in the corresponding adipose-cell lysate. **b** Adipocytes that were isolated form visceral fat of LETO and OLETF rats were cultured for 3 days and the culture supernatants were collected every 24 h. The EV fractions were collected by ultracentrifugation, and the cells were lysed

levels in the exosomal proteome, according to quantitative proteomic analysis.

We demonstrated changes in the expression of many kinds of proteins (128 upregulated and 72 downregulated) in the exosomes of diabetic rats. These differentially expressed proteins in the adipocytic exosomes isolated from OLETF and LETO rats include caveolin 1 (upregulated in OLETF rats), lipoprotein lipase (upregulated in OLETF rats), aquaporin 7 (upregulated in OLETF rats), adenylate kinase 2 (downregulated in OLETF rats), catalase (downregulated in OLETF rats), and liver carboxylesterase (downregulated in OLETF rats). Some authors suggested that caveolin 1 is involved in the pathogenesis of obesity and adipose-tissue-related insulin signaling in humans [40, 41]. Upregulation of caveolin 1 mRNA expression was reported in obese patients with type 2 diabetes compared to lean controls [40]. Lipoprotein lipase performs a major function in the metabolism and transport of lipids and is the enzyme responsible for hydrolysis of core triglycerides [42]. Furthermore, upregulation of mRNA expression of lipoprotein lipase was shown in visceral adipose tissue of OLETF rats compared to LETO rats [43]. Moreover, 1 study demonstrated that a reduced lipoprotein lipase amount and activity correlate inversely with the extent of visceral fat accumulation.

Aquaporin 7 is a glycerol channel mainly expressed in adipocytes [44, 45]. Recently, an increase (2.5-fold) of mRNA expression of aquaporin 7 was demonstrated in

adipose tissue of OLETF rats compared to LETO rats [44]. AK2, a mitochondrial enzyme, regulates adenine nucleotide interconversion. Upregulation of the AK2 protein is strongly associated with adipocytic differentiation [46]. In our study, the exosomes and adipose cells show a lower level of the AK2 protein expression in OLETF rats compared to LETO rats. This finding can be explained as follows: downregulation of AK2 causes perturbation of energy metabolism in mitochondria.

Catalase is an antioxidant enzyme expressed in various tissues; it protects cells from harmful effects of hydrogen peroxide by converting it to oxygen and water [47]. In adipose tissue of obese mice, expression of catalase significantly decreases [48] just as in our present proteomic and western blot analysis. It was also reported that the activity of catalase decreases during oxidative stress judging by lipid peroxide content of the renal cortex in OLETF rats [47]. Although liver carboxylesterase (carboxylesterase 1) has not been detected in adipose tissue of OLETF rats, carboxylesterase 1/esterase-x-deficient mice become obese and hyperlipidemic and develop hepatic steatosis even on a standard diet [49, 50]. Some researchers showed that phosphorylation of AKT, which is a downstream kinase of insulin signaling, is significantly reduced in adipose tissue of carboxylesterase 1/esterase-x-deficient mice [50]. We can theorize that the weaker expression of liver carboxylesterase in adipocytes of OLETF rats is indicative of insulin resistance.

We can conclude that our proteomic analysis and bioinformatic search can provide a means for gathering comprehensive data on exosomal proteins in diabetes. Ours seems to be the first report on proteomic characterization of adipocytic exosomes from obese rats with or without diabetes (OLETF and LETO). Our results support the utility of protein profiling of adipose-tissue-derived exosomes and suggest that diseased-tissue exosomes reflect the status and functions of the tissue of origin. Moreover, independent confirmation of our findings should advance the understanding of obesity- and diabetes-related diseases.

Acknowledgments This work was supported by the grant of Basic Science Research Program through the National Research Foundation of Korea (NRF) funded by the Ministry of Education, Science and Technology (2010-0022811 to M.C.B.) and the National Research Foundation of Korea (NRF) grant funded by the Korea government (2014R1A5A2009242 to M.C.B.) and the National Research Foundation of Korea (NRF) grant (NRF-2013R1A6A3A01024597 to P.G.M.).

Conflict of interest The authors declare that they have no conflict of interests.

Ethical approval All procedures performed in studies involving animals were in accordance with protocols approved by Kyungpook National University (KNU) Institutional Animal Care and Use Committees (IACUCs).

References

1. Skog J, Wurdinger T, van Rijn S, Meijer DH, Gainche L, Sena-Esteves M, Curry WT Jr, Carter BS, Krichevsky AM, Breakefield XO (2008) Glioblastoma microvesicles transport RNA and proteins that promote tumour growth and provide diagnostic biomarkers. Nat Cell Biol 10(12):1470–1476. doi:10.1038/ncb1800
2. Valadi H, Ekstrom K, Bossios A, Sjostrand M, Lee JJ, Lotvall JO (2007) Exosome-mediated transfer of mRNAs and microRNAs is a novel mechanism of genetic exchange between cells. Nat Cell Biol 9(6):654–659. doi:10.1038/ncb1596
3. Deng ZB, Poliakov A, Hardy RW, Clements R, Liu C, Liu Y, Wang J, Xiang X, Zhang S, Zhuang X, Shah SV, Sun D, Michalek S, Grizzle WE, Garvey T, Mobley J, Zhang HG (2009) Adipose tissue exosome-like vesicles mediate activation of macrophage-induced insulin resistance. Diabetes 58(11): 2498–2505. doi:10.2337/db09-0216
4. Gross JC, Chaudhary V, Bartscherer K, Boutros M (2012) Active Wnt proteins are secreted on exosomes. Nat Cell Biol 14(10):1036–1045. doi:10.1038/ncb2574
5. Luga V, Zhang L, Viloria-Petit AM, Ogunjimi AA, Inanlou MR, Chiu E, Buchanan M, Hosein AN, Basik M, Wrana JL (2012) Exosomes mediate stromal mobilization of autocrine Wnt-PCP signaling in breast cancer cell migration. Cell 151(7):1542–1556. doi:10.1016/j.cell.2012.11.024
6. Peinado H, Aleckovic M, Lavotshkin S, Matei I, Costa-Silva B, Moreno-Bueno G, Hergueta-Redondo M, Williams C, Garcia-Santos G, Ghajar C, Nitadori-Hoshino A, Hoffman C, Badal K, Garcia BA, Callahan MK, Yuan J, Martins VR, Skog J, Kaplan RN, Brady MS, Wolchok JD, Chapman PB, Kang Y, Bromberg J, Lyden D (2012) Melanoma exosomes educate bone marrow progenitor cells toward a pro-metastatic phenotype through MET. Nat Med 18(6):883–891. doi:10.1038/nm.2753
7. Moon PG, You S, Lee JE, Hwang D, Baek MC (2011) Urinary exosomes and proteomics. Mass Spectrom Rev 30(6):1185–1202. doi:10.1002/mas.20319
8. Antonyak MA, Li B, Boroughs LK, Johnson JL, Druso JE, Bryant KL, Holowka DA, Cerione RA (2011) Cancer cell-derived microvesicles induce transformation by transferring tissue transglutaminase and fibronectin to recipient cells. Proc Natl Acad Sci USA 108(12):4852–4857. doi:10.1073/pnas.1017667108
9. Sano S, Izumi Y, Yamaguchi T, Yamazaki T, Tanaka M, Shiota M, Osada-Oka M, Nakamura Y, Wei M, Wanibuchi H, Iwao H, Yoshiyama M (2014) Lipid synthesis is promoted by hypoxic adipocyte-derived exosomes in 3T3-L1 cells. Biochem Biophys Res Commun 445(2):327–333. doi:10.1016/j.bbrc.2014.01.183
10. Muller G, Jung C, Straub J, Wied S, Kramer W (2009) Induced release of membrane vesicles from rat adipocytes containing glycosylphosphatidylinositol-anchored microdomain and lipid droplet signalling proteins. Cell Signal 21(2):324–338. doi:10.1016/j.cellsig.2008.10.021
11. Muller G, Schneider M, Biemer-Daub G, Wied S (2011) Microvesicles released from rat adipocytes and harboring glucosylphosphatidylinositol-anchored proteins transfer RNA stimulating lipid synthesis. Cell Signal 23(7):1207–1223. doi:10.1016/j.cellsig.2011.03.013
12. Phoonsawat W, Aoki-Yoshida A, Tsuruta T, Sonoyama K (2014) Adiponectin is partially associated with exosomes in mouse serum. Biochem Biophys Res Commun 448(3):261–266. doi:10.1016/j.bbrc.2014.04.114
13. Wellen KE, Hotamisligil GS (2005) Inflammation, stress, and diabetes. J Clin Investig 115(5):1111–1119. doi:10.1172/JCI25102
14. Kershaw EE, Flier JS (2004) Adipose tissue as an endocrine organ. The Journal of clinical endocrinology and metabolism 89(6):2548–2556. doi:10.1210/jc.2004-0395

15. Scherer PE (2006) Adipose tissue: from lipid storage compartment to endocrine organ. Diabetes 55(6):1537–1545. doi:10.2337/db06-0263
16. Kannel WB, Cupples LA, Ramaswami R, Stokes J 3rd, Kreger BE, Higgins M (1991) Regional obesity and risk of cardiovascular disease; the Framingham Study. J Clin Epidemiol 44(2):183–190
17. Maeda K, Okubo K, Shimomura I, Mizuno K, Matsuzawa Y, Matsubara K (1997) Analysis of an expression profile of genes in the human adipose tissue. Gene 190(2):227–235
18. Hotamisligil GS, Shargill NS, Spiegelman BM (1993) Adipose expression of tumor necrosis factor-alpha: direct role in obesity-linked insulin resistance. Science 259(5091):87–91
19. Kobayashi K (2005) Adipokines: therapeutic targets for metabolic syndrome. Curr Drug Targets 6(4):525–529
20. Matsuzawa Y (2005) White adipose tissue and cardiovascular disease. Best Pract Res Clin Endocrinol Metabol 19(4):637–647. doi:10.1016/j.beem.2005.07.001
21. Lehr S, Hartwig S, Lamers D, Famulla S, Muller S, Hanisch FG, Cuvelier C, Ruige J, Eckardt K, Ouwens DM, Sell H, Eckel J (2012) Identification and validation of novel adipokines released from primary human adipocytes. Mol Cell Proteomics : MCP 11(1):M111 010504. doi:10.1074/mcp.M111.010504
22. Ishida K, Mizuno A, Min Z, Sano T, Shima K (1995) Which is the primary etiologic event in Otsuka Long-Evans Tokushima Fatty rats, a model of spontaneous non-insulin-dependent diabetes mellitus, insulin resistance, or impaired insulin secretion? Metab Clin Exp 44(7):940–945
23. Kawano K, Hirashima T, Mori S, Saitoh Y, Kurosumi M, Natori T (1992) Spontaneous long-term hyperglycemic rat with diabetic complications. Otsuka Long-Evans Tokushima Fatty (OLETF) strain. Diabetes 41(11):1422–1428
24. Kawano K, Hirashima T, Mori S, Natori T (1994) OLETF (Otsuka Long-Evans Tokushima Fatty) rat: a new NIDDM rat strain. Diabetes Res Clin Pract 24(Suppl):S317–S320
25. Muller G, Ertl J, Gerl M, Preibisch G (1997) Leptin impairs metabolic actions of insulin in isolated rat adipocytes. J Biol Chem 272(16):10585–10593
26. Cho YE, Singh TS, Lee HC, Moon PG, Lee JE, Lee MH, Choi EC, Chen YJ, Kim SH, Baek MC (2012) In-depth identification of pathways related to cisplatin-induced hepatotoxicity through an integrative method based on an informatics-assisted label-free protein quantitation and microarray gene expression approach. Mol Cell Proteomics MCP 11(1):M111 010884. doi:10.1074/mcp.M111.010884
27. Lee JE, Park JH, Moon PG, Baek MC (2013) Identification of differentially expressed proteins by treatment with PUGNAc in 3T3-L1 adipocytes through analysis of ATP-binding proteome. Proteomics 13(20):2998–3012. doi:10.1002/pmic.201200549
28. Tsou CC, Tsai CF, Tsui YH, Sudhir PR, Wang YT, Chen YJ, Chen JY, Sung TY, Hsu WL (2010) IDEAL-Q, an automated tool for label-free quantitation analysis using an efficient peptide alignment approach and spectral data validation. Mol Cell Proteomics MCP 9(1):131–144. doi:10.1074/mcp.M900177-MCP200
29. Moon PG, Kwack MH, Lee JE, Cho YE, Park JH, Hwang D, Kim MK, Kim JC, Sung YK, Baek MC (2013) Proteomic analysis of balding and non-balding mesenchyme-derived dermal papilla cells from androgenetic alopecia patients using on-line two-dimensional reversed phase-reversed phase LC-MS/MS. J Proteomics 85:174–191. doi:10.1016/j.jprot.2013.04.004
30. Muller G, Jung C, Wied S, Biemer-Daub G (2009) Induced translocation of glycosylphosphatidylinositol-anchored proteins from lipid droplets to adiposomes in rat adipocytes. Br J Pharmacol 158(3):749–770. doi:10.1111/j.1476-5381.2009.00360.x
31. Kim HS, Choi DY, Yun SJ, Choi SM, Kang JW, Jung JW, Hwang D, Kim KP, Kim DW (2012) Proteomic analysis of microvesicles derived from human mesenchymal stem cells. J Proteome Res 11(2):839–849. doi:10.1021/pr200682z
32. Hwang HH, Moon PG, Lee JE, Kim JG, Lee W, Ryu SH, Baek MC (2011) Identification of the target proteins of rosiglitazone in 3T3-L1 adipocytes through proteomic analysis of cytosolic and secreted proteins. Mol Cells 31(3):239–246. doi:10.1007/s10059-011-0026-6
33. Ertunc ME, Sikkeland J, Fenaroli F, Griffiths G, Daniels MP, Cao H, Saatcioglu F, Hotamisligil GS (2015) Secretion of fatty acid binding protein aP2 from adipocytes through a nonclassical pathway in response to adipocyte lipase activity. J Lipid Res 56(2):423–434. doi:10.1194/jlr.M055798
34. Aoki N, Yokoyama R, Asai N, Ohki M, Ohki Y, Kusubata K, Heissig B, Hattori K, Nakagawa Y, Matsuda T (2010) Adipocyte-derived microvesicles are associated with multiple angiogenic factors and induce angiogenesis in vivo and in vitro. Endocrinology 151(6):2567–2576. doi:10.1210/en.2009-1023
35. Muller G, Schneider M, Biemer-Daub G, Wied S (2011) Upregulation of lipid synthesis in small rat adipocytes by microvesicle-associated CD73 from large adipocytes. Obesity 19(8):1531–1544. doi:10.1038/oby.2011.29
36. Koeck ES, Iordanskaia T, Sevilla S, Ferrante SC, Hubal MJ, Freishtat RJ, Nadler EP (2014) Adipocyte exosomes induce transforming growth factor beta pathway dysregulation in hepatocytes: a novel paradigm for obesity-related liver disease. J Surg Res 192(2):268–275. doi:10.1016/j.jss.2014.06.050
37. Shono S, Kose H, Yamada T, Matsumoto K (2007) Proteomic analysis of a diabetic congenic rat identified age-dependent alteration of an acidic protein. J Med Investig JMI 54(3–4):289–294
38. Nakatani S, Kakehashi A, Ishimura E, Yamano S, Mori K, Wei M, Inaba M, Wanibuchi H (2011) Targeted proteomics of isolated glomeruli from the kidneys of diabetic rats: sorbin and SH3 domain containing 2 is a novel protein associated with diabetic nephropathy. Exp Diabetes Res 2011:979354. doi:10.1155/2011/979354
39. Oh-Ishi M, Satoh M, Maeda T (2000) Preparative two-dimensional gel electrophoresis with agarose gels in the first dimension for high molecular mass proteins. Electrophoresis 21(9):1653–1669. doi:10.1002/(SICI)1522-2683(20000501)21:9<1653:AID-ELPS1653>3.0.CO;2-9
40. Catalan V, Gomez-Ambrosi J, Rodriguez A, Silva C, Rotellar F, Gil MJ, Cienfuegos JA, Salvador J, Fruhbeck G (2008) Expression of caveolin-1 in human adipose tissue is upregulated in obesity and obesity-associated type 2 diabetes mellitus and related to inflammation. Clin Endocrinol 68(2):213–219. doi:10.1111/j.1365-2265.2007.03021.x
41. Otsu K, Toya Y, Oshikawa J, Kurotani R, Yazawa T, Sato M, Yokoyama U, Umemura S, Minamisawa S, Okumura S, Ishikawa Y (2010) Caveolin gene transfer improves glucose metabolism in diabetic mice. Am J Physiol Cell Physiol 298(3):C450–C456. doi:10.1152/ajpcell.00077.2009
42. Wang H, Eckel RH (2009) Lipoprotein lipase: from gene to obesity. Am J Physiol Endocrinol Metab 297(2):E271–E288. doi:10.1152/ajpendo.90920.2008
43. Hida K, Wada J, Zhang H, Hiragushi K, Tsuchiyama Y, Shikata K, Makino H (2000) Identification of genes specifically expressed in the accumulated visceral adipose tissue of OLETF rats. J Lipid Res 41(10):1615–1622
44. Lee DH, Park DB, Lee YK, An CS, Oh YS, Kang JS, Kang SH, Chung MY (2005) The effects of thiazolidinedione treatment on the regulations of aquaglyceroporins and glycerol kinase in OLETF rats. Metab Clin Exp 54(10):1282–1289. doi:10.1016/j.metabol.2005.04.015

45. Rodriguez A, Catalan V, Gomez-Ambrosi J, Fruhbeck G (2006) Role of aquaporin-7 in the pathophysiological control of fat accumulation in mice. FEBS Lett 580(20):4771–4776. doi:10.1016/j.febslet.2006.07.080
46. Burkart A, Shi X, Chouinard M, Corvera S (2011) Adenylate kinase 2 links mitochondrial energy metabolism to the induction of the unfolded protein response. J Biol Chem 286(6):4081–4089. doi:10.1074/jbc.M110.134106
47. Sugimoto K, Tsuruoka S, Fujimura A (2001) Effect of enalapril on diabetic nephropathy in OLETF rats: the role of an anti-oxidative action in its protective properties. Clin Exp Pharmacol Physiol 28(10):826–830
48. Okuno Y, Matsuda M, Kobayashi H, Morita K, Suzuki E, Fukuhara A, Komuro R, Shimabukuro M, Shimomura I (2008) Adipose expression of catalase is regulated via a novel remote PPARgamma-responsive region. Biochem Biophys Res Commun 366(3):698–704. doi:10.1016/j.bbrc.2007.12.001
49. Quiroga AD, Lian J, Lehner R (2012) Carboxylesterase1/Esterase-x regulates chylomicron production in mice. PLoS One 7(11):e49515. doi:10.1371/journal.pone.0049515
50. Quiroga AD, Li L, Trotzmuller M, Nelson R, Proctor SD, Kofeler H, Lehner R (2012) Deficiency of carboxylesterase 1/esterase-x results in obesity, hepatic steatosis, and hyperlipidemia. Hepatology 56(6):2188–2198. doi:10.1002/hep.25961